

Complexity versus Simplicity:

An Example of Groundwater Model Ranking with the Akaike

Information Criterion

Engelhardt, I.^{1), 2)*}, De Aguinaga, J.G.³⁾, Mikat, H.⁴⁾,

Schüth, C.^{1).}, Lenz, O.¹⁾, Liedl, R.⁵⁾

1) Technische Universität Darmstadt, Institute of Applied Geosciences, Germany

2) Forschungszentrum Jülich, Institute of Bio- and Geosciences, Germany

3) Bauhaus-Universität Weimar, Research Training Group, Germany

4) Hessenwasser GmbH & Co. KG, Germany

5) Technische Universität Dresden, Institute for Groundwater Management, Germany

*Corresponding author address: i.engelhardt@fz-juelich.de

Abstract

A groundwater model characterized by a lack of field data to estimate hydraulic model parameters and boundary conditions combined with many piezometric head observations was investigated concerning model uncertainty. Different conceptual models with a stepwise increase from 0 to 30 adjustable parameters were calibrated using PEST. Residuals, sensitivities, the Akaike Information Criterion (AIC and AICc), Bayesian Information Criterion (BIC), and Kashyap's Information Criterion (KIC) were calculated for a set of seven inverse calibrated models with increasing complexity by gradually rising the number of adjustable model parameters. Finally, the likelihood of each model was computed. As expected, residuals and standard errors decreased with an increasing amount of adjustable model parameters. The model with only 15 adjusted parameters was evaluated by AIC as the best option with a likelihood of 98 %, while the model based on sedimentological information obtained the worst AIC value. BIC and KIC selected a simpler model than the model chosen by AIC as optimal. Computing of AIC, BIC, and KIC

28 yielded the most important information to assess the model likelihood. Comparing only
29 residuals of different conceptual models was less valuable and would result in an
30 overparameterization and certainty loss in the conceptual model approach. Sensitivities of
31 piezometric heads were highest for the model with five adjustable parameters following
32 distinctively changes of extracted groundwater volumes. With increasing amount of
33 adjustable parameters piezometric heads became less sensitive for the model calibration
34 and remained constant during the simulated period. With increasing freedom model
35 parameters lost their impact on the model response. Additionally, using only
36 sedimentological data to derive hydraulic parameters possessed a consistent error into
37 the simulation results and cannot recommended generating a true and valuable model.

38

39 *Keywords: AIC, BIC, KIC, Sensitivity, Uncertainty, PEST*

40

41 **1. Introduction**

42 Uncertainty is a key issue in hydrogeological modeling. Uncertainties are
43 associated with parameter values, chosen scale, data quality, validity of
44 boundaries, and initial conditions. Moreover, groundwater models are subject to
45 several errors resulting from conceptual and stochastic uncertainty. Uncertainty in
46 calibrated parameters can originate from inaccuracies in field data, insensitivity
47 with regard to changes in model parameters, and correlations within adjusted
48 parameter sets (Singh et al., 2010). In many cases, measured field or laboratory
49 data cannot be directly used to parameterize the model since they are collected at
50 different temporal or spatial scale. Overparameterized models increase
51 uncertainty since the information of the observations is distributed through all the

52 parameters. To simulate a natural system with a numerical model, data have to
53 be filtered, averaged and modified. A way to reduce this uncertainty is to select a
54 *parsimonious model*, which provides good performance with as few calibrated
55 parameters as possible.

56 There are several approaches to find this compromise between model fit and low
57 number of calibration parameters (Hill and Tiedeman, 2007, Massmann et al.
58 2006). One of these approaches is the Akaike Information Criterion (AIC; Akaike,
59 1973). AIC is a probabilistic criterion based on the maximum likelihood theory and
60 treats the problem of parsimonious model selection as an optimization problem
61 across a set of proposed conceptual models (Burnham and Anderson, 2002). In
62 addition, AIC allows the ranking of models and determines the optimal model for a
63 given data set. It identifies wherever the results of the selected model are already
64 satisfactory or wherever an increased effort is needed by introducing more
65 parameters into a model, so that AIC is able to select a more complicated model
66 with a better fit to the observed data.

67 The application of the AIC is relatively new in groundwater modeling and still not
68 standard, although it has been applied in several studies (e.g., Foglia et al., 2007;
69 Hill, 2006; Hill and Tiedeman, 2007; Katumba et al., 2008; Parker et al., 2010;
70 Poeter and Anderson, 2005; Singh et al., 2010; and Ye et al., 2010). Foglia et al.
71 (2007) uses piezometric pressure heads and stream flow gauges for a
72 groundwater model with a huge area of that were monitored over some month
73 and calibrates the hydraulic conductivity. Poeter and Anderson (2005) analyzed
74 synthetic data sets, Katumba et al. (2008) investigates the likelihood of models of
75 tank experiments, and Parker et al. (2010) analyzes two impeller flow loggings.

76 Singh et al. (2010) and Ye et al. (2010) compared the model uncertainty with
77 respect to the estimated recharge for the Yucca Mountain nuclear waste
78 repository that is well documented over decades of years. In this study, a typical
79 field-generated data set, as often available for numerical investigations for
80 groundwater management issues was investigated. The data set suffers from a
81 lack of information on boundary and initial conditions, however, observation data
82 were collected in great quantities and over a long-term. Information criteria, such
83 as the AIC, might be helpful to define the best model concept with respect to the
84 model performance and uncertainty.

85 The investigated groundwater model was based on very few data available from
86 pumping tests giving hydraulic properties of the aquifer and most hydraulic
87 parameters had to be estimated from sedimentological investigations.
88 Sedimentological information was derived from borehole drillings conducted more
89 than 100 years ago and was associated with high uncertainties. On the other
90 hand, long-term data, in form of high resolution groundwater level time series,
91 were provided for the model calibration. In this study, the uncertainty of different
92 model approaches was addressed by gradually increasing the amount of
93 adjustable model parameters to predict measured groundwater fluctuations.
94 Finally, the optimal model selected by different information criteria (Akaike's
95 Information Criterion, AIC and AICc, Bayesian Information Criterion, BIC, and
96 Kashyap's Information Criterion, KIC) were evaluated considering the calibration
97 results and the parameter uncertainties of the model.

98

100 **2. Materials and Methods**

101 **2.1 Investigated Field Site**

102 *Geological Setting*

103 The study area is situated south of the city of Frankfurt and east of the Frankfurt
104 International Airport in the German federal state Hesse. The site is located in the
105 northern part of the Upper Rhine Graben (URG), which is part of the European
106 Cenozoic Rift System (Ziegler and Dèzes, 2005). The URG, an approximately
107 300 km long and 40 km wide elongate lowland is flanked by uplift plateaus and
108 terminated in the northern part by the WSW – ESE striking southern boundary
109 fault of the Rhenish Massif, bounded to the West by the Mainz basin and to the
110 East by the Hanau basin and the Odenwald Massif (*Fig 1a*). The graben-filling
111 sediments are of Eocene to Early Miocene and of Plio-/Pleistocene age (Berger et
112 al., 2005). The subsidence of the graben resulted in up to 2000 m thick Tertiary
113 deposits and more than 100 m thick fluvial Quaternary sediments (Anderle, 1968;
114 Bartz, 1974). In the northernmost part of the URG between Mörfelden, Langen,
115 Frankfurt, and the Lower Main area mainly fluvial sand and gravel with embedded
116 clay lenses were deposited during the Pleistocene (Anderle, 1968). The
117 thicknesses of these deposits in the northern offset of the URG range between 10
118 and 40 m (*Fig 1b*). Holocene eolian silty fine sand was deposited on top of this
119 layer. The base of the Quaternary and Tertiary sand and gravel consists of
120 Permian sandstone and conglomerates as well as Tertiary basalt.

123 Average groundwater flow velocities within the Quaternary and Tertiary sand and
124 gravel deposits are about 0.5 m/d and groundwater flows from the Sprendlinger
125 Horst in the South-East towards the river Main. The depth to the groundwater
126 table varies between 3 and 5 m near the river Main and gradually increases up to
127 15 m towards the South and East.

128

129 ***Fig. 1: a) Simplified geological map showing the northern part of the Upper***
130 ***Rhine Graben, the adjacent Mainz and Hanau basins (modified after***
131 ***Lahner and Toloczyki (2004); W: Wiesbaden, M: Mainz, F: Frankfurt, H:***
132 ***Heidelberg). b) Thickness of the Quaternary sand and gravel deposits***
133 ***south of Frankfurt (after Anderle, 1968; Bartz, 1974; Anderle and***
134 ***Golwer, 1980). Location of the model domain, the water works, and of***
135 ***transect A-B.***

136

137 The long-term precipitation (1961-1993) averages around 675 mm/a as measured
138 at the meteorological station in Frankfurt. About 15% of the precipitation, thus 100
139 to 150 mm/a, can infiltrate into the groundwater (Berthold & Hergesell, 2005). The
140 groundwater within this area is intensively used for drinking water and industrial
141 purposes. Several water works are located within this region. In the water works
142 Oberforsthaus, located directly in the study area, 18 production wells were
143 operated. Groundwater extraction started already in 1894. About 100 years later,
144 the water works was rebuilt and then extraction rates increased within a few years
145 from 560,000 m³/a (1995) to 1.4*10⁶ m³/a in 2000. Since 2005, the water works
146 has been kept in stand-by operation. For sustainable groundwater management
147 issues groundwater resources were recharged with treated water from the river
148 Main to prevent an excessive groundwater table drop. Surface water was

149 infiltrated by horizontal pipes and a small pond (named Jacobi-pond). During
150 periods of high groundwater extraction rates treated surface water infiltration
151 reached up to 35 to 40% of the extracted groundwater volume and was reduced
152 to about 25% in periods with average extraction rates. The artificial groundwater
153 recharge stopped in 2005, when the water works changed to stand-by operation.

154

155 **2.2 Numerical Model Set-up**

156 *Discretization*

157 The geological structure of the investigated Quaternary aquifer consists of a
158 complex system of high and low permeable layers. Nine lithological units were
159 identified in the borehole drillings. For translation of the complex geological
160 information into a numerical model some simplifications were necessary. All
161 geological information obtained from drillings and geological maps were
162 summarized into three hydrostratigraphic layer (*Fig. 2*): (i) dominated by high
163 permeable aquifer material (gravel and coarse sand), (ii) dominated by medium
164 and low permeable aquifer material (medium and fine sand), and (iii) a deeper
165 layer dominated again by high permeable material (gravel and coarse sand). The
166 impermeable aquifer base is built of silt, clay, sandstone, limestone, or basalt.
167 Then, 15 profiles were constructed containing these three hydrostratigraphic
168 layer. Geological information between the profiles were interpolated to estimate
169 the top and bottom of the three hydrostratigraphic layer (*Fig. 2*).

170 With these simplifications the spatial discretization contained 22,680 grid cells.

171 The temporal discretization for the simulated period of 19 years, ranging between

172 1990 and 2009, included 379 stress periods to capture the monthly collected
173 piezometric pressure heads.

174

175 ***Fig 2: Averaged hydrostratigraphic layer from nine lithologic units along***
176 ***transect A-B.***

177

178 *Hydraulic Properties*

179 Only very few data were available about hydraulic conductivities and storage of
180 the aquifer layers. Within a layer, several micro layers may be present and an
181 averaging technique was applied to account for these heterogeneities. First, all
182 data obtained from the geological description of the borehole data were used to
183 assign an initial estimate on hydraulic conductivities and storage coefficients to
184 each of the nine lithological units. For each of the three hydrostratigraphic layer
185 an equivalent hydraulic conductivity and storage coefficient was calculated to
186 account for the contribution of the lithological units within each hydrostratigraphic
187 layer, respectively (*Fig. 3*).

188

189 ***Fig. 3: Averaging technique to derive the equivalent hydraulic***
190 ***conductivities around two wells within the three hydrostratigraphic***
191 ***layer that contain nine lithologic units.***

192

193 As an example, the equivalent hydraulic conductivity (K_{eq}) of hydrostratigraphic
194 layer 1 around well A was obtained by calculating the weighted arithmetic
195 average of the lithological units with:

196
$$K_{eq,1} = \frac{d1A \cdot K_{gravel} + d2A \cdot K_{coarse\ sand} + d3A \cdot K_{fine\ sand} + d4A \cdot K_{gravel}}{d1A + d2A + d3A + d4A} \quad (1)$$

197 *with $K_{eq,1}$ = Equivalent hydraulic conductivity of layer 1*

198 *dA = Thickness of the lithological unit in the respective*
 199 *hydrostratigraphic layer at well A*

200 *1,2,... = Number of the lithological unit*

201 *K = Hydraulic conductivity estimated from the sedimentological*
 202 *description of the lithological unit*

203

204 Equivalent hydraulic conductivities and storage values were interpolated over the
 205 model domain for each of the three hydrostratigraphic layers and subdivided into
 206 ten conductivity and storage zones, respectively (Fig. 4). Hydraulic conductivity
 207 and storage zones showed a different pattern and frequency in each of the three
 208 layers or were not developed at all. The interpolation of the equivalent hydraulic
 209 conductivity zones failed around geological structures such as faults. Therefore,
 210 a final manual adjustment of the hydraulic parameters to maintain relevant
 211 geological features was necessary.

212

213 **Fig. 4: Spatial distribution of the ten equivalent hydraulic conductivities of**
 214 **Model 1 (uncalibrated model based on sedimentological information)**
 215 **within the three hydrostratigraphic layer.**

216

217 *Numerical Model Boundaries*

218 The standard finite-difference model MODFLOW (Harbaugh et al., 2005) was
 219 used for the flow simulations. Groundwater levels measured in 1990 within 47
 220 observation wells were interpolated and used as initial head distribution (Fig. 5).

221 The main inflow into the groundwater system is recharge that varied monthly
222 during the investigated 20 years. Further groundwater inflow was caused by
223 surface water infiltration from the Jacobi Pond. Groundwater outflow mainly
224 occurred by exfiltration into the river Main (*Fig. 5*). The stage of the river Main
225 was adjusted monthly during the investigated period by applying a linear
226 interpolation between two hydrological stations close to the model domain:
227 Frankfurt Osthafen (4 km upstream) and Raunheim (16 km downstream). The
228 water level of the Jacobi Pond was assumed to remain constant during the
229 investigated period since groundwater levels measured near the pond remained
230 fairly constant. Leakage between groundwater and surface water is driven by the
231 gradient between the surface water stage and the groundwater, and the
232 conductivity of the river bed and Jacobi Pond bottom sediments. The stage of the
233 surface water was prescribed during the simulations, while the hydraulic
234 conductivities of the river bed and Jacobi Pond sediments were adjusted in an
235 initial manual “pre-calibration”. Along the South-West boundary, groundwater
236 flowed out of the model domain towards the water works Goldstein, which started
237 operation in 1995. This subsurface outflow was accounted for by a general head
238 boundary. The piezometric head outside of the model domain was given by the
239 monthly measured groundwater level at the pumping wells of the water works
240 Goldstein. Within the model domain the water works Oberforsthaus operated
241 about 18 pumping wells between 1990 and 2005. The monthly measured
242 extraction rates were corrected by the injected artificial recharge, and resulting
243 extraction volumes were assigned at the water works location.

244

245 **Fig. 5: Boundary conditions, initial head distribution of the numerical flow**
246 **model and location of the observation well groups.**

247
248 *Model Calibration*

249 The non-linear parameter estimator PEST (Doherty, 2010) was used for the
250 automated model calibration through an inverse parameter estimation process
251 based on the Gauss-Marquardt-Levenberg method. PEST minimizes
252 discrepancies between model simulated outputs and the corresponding
253 measurements by minimizing the weighted sum of squared differences between
254 the respective values. PEST also computes the sensitivities with regard to
255 selected parameters at all observation points. These sensitivities provide a
256 measure of how much a simulated value changes in response to a perturbation
257 of an adjustable parameter (Hill & Tiedeman, 2007).

258 In PEST the composite sensitivity s_i of a parameter i is computed with (Doherty,
259 2010):

260
$$s_i = (\mathbf{J}^t \mathbf{Q} \mathbf{J})_{ii}^{1/2} / m \quad (2)$$

261 where \mathbf{J} is the Jacobian matrix, \mathbf{Q} is the weight matrix, $\mathbf{J}^t \mathbf{Q} \mathbf{J}$ is the normal matrix,
262 and m is the number of observations with non-zero weights.

263
264 The composite observation sensitivity s_j of observation j is computed in PEST
265 with (Doherty, 2010):

266
$$s_j = \{\mathbf{Q} (\mathbf{J}^t \mathbf{J})\}_{jj}^{1/2} / n \quad (3)$$

267 where $\mathbf{J}^t \mathbf{J}$ is the Hessian matrix, j is the counter of the observations, and n is the
268 number of adjustable parameters.

269

270 Piezometric heads collected at 41 observation wells between 1990 and 2009
271 were used for the model calibration giving a total number of 5,081 observation
272 points (*Fig. 5*). For a better overview, observation wells were categorized into six
273 groups: (i) near Jacobi Pond, (ii) near the River Main, (iii) Southern area, (iv)
274 Western area, (v) Northern area, and, (vi), around the water works Oberforsthaus
275 (*Fig. 5*) to account for the different factors influencing the hydraulic pattern of the
276 investigated region. Hydraulic conductivities and storage coefficients were
277 estimated using PEST. First guesses of these parameters were assigned as
278 derived from sedimentological interpretation of the borehole data (*Fig. 3 and Fig.*
279 *4*).

280 Composite observation sensitivity s_j were computed for each observation point to
281 be an overall measure of the sensitivity of all 5,081 observation points to all
282 adjustable parameter in the model, respectively.

283 After calibration of the hydraulic parameters a validation was conducted with the
284 optimal model selected by the information criterion. This validation analyzed
285 piezometric pressure heads measured at six further observation wells
286 representing each observation group. These observation wells were not used in
287 the prior parameter estimation during the inverse modeling. This procedure was
288 chosen due to the analysis of Bredehoeft and Konikow (2012). They emphasize
289 that a professional judgment of the model is only possible using historical data,
290 while the validation of the model against future response remains challenging.
291 However, errors resulting from conceptual errors will neither be addressed by
292 using historical nor future data in the validation (Bredehoeft and Konikow, 2012).

293

294

2.3 Principles to Weight and Rank Models using AIC, AICc, BIC, and KIC

Akaike's Information Criterion

Computation of the AIC allows the selection of a parsimonious model that uses the smallest number of parameters needed to provide an adequate approximation to the measured data. Thus, a compromise between a “good” fit and a small number of parameters can be found.

Akaike (Akaike, 1973) defined a model selection criterion called Akaike's Information Criterion (AIC) that is based on the estimation of the information loss between an approximating model and an unknown parametrized truth. AIC is defined as follows (Ye et al., 2008):

$$AIC = n \ln(\hat{\sigma}_{ML}^2) + n \ln(2\pi) + n + \ln |Q^{-1}| + 2p \quad (4)$$

where p equals the number of estimated model parameters plus one, n is the number of observations, Q is the weight matrix, and $\hat{\sigma}_{ML}^2$ represents an estimate of the variance of weighted residuals, which is given by:

$$\hat{\sigma}_{ML}^2 = \frac{\sum_{j=1}^n (\varepsilon q)_i^2}{n} \quad (5)$$

where ε stands for the residuals (observed minus calculated values), and q is the weight of the j^{th} observation, respectively, which is always one for the present study.

The first term in Eq. 4 represents the lack of the model fit, which decreases when more parameters are included. The last term can be seen as “penalty” term for incorporating more parameters as this term increases within rising amount of

316 adjustable parameters.

317 The two middle terms are constants for a specific data set, and are not affected if
318 parameters are added or removed from the models (Cavanaugh, 1997). Weights
319 were set to one since no information about data uncertainty and measurement
320 error was available. However, when additional information about confidence of
321 the data is available the weight matrix of Eq. 4 allows comparing models based
322 on a weighted data set of observations. This reflects the confidence to specific
323 measurements, or simply, provides the flexibility to scale observations according
324 to additional information or normalization procedures (Hill and Tiedeman, 2002).

325 Akaike (1978) defined weights w_j to obtain a relative measure of the likelihood of
326 a model for a given set of N models. These weights are expressed as:

$$327 \quad w_j = \exp(-0.5\Delta_j) / \sum_{j=1}^N \exp(-0.5\Delta_j) \quad (6)$$

328 where j is the counter of models, and $\Delta_j = AIC_j - AIC_{min}$ denotes the AIC
329 difference to the smallest AIC of all considered models.

330 The larger the AIC difference of a model, the less likely it is to be the best one.

331

332 *Alternative Information Criteria*

333 Several modifications of AIC have been developed. For the case of having a
334 small sample, $n/K < 40$, Burnham and Anderson (2002) suggest using AIC_c :

$$335 \quad AIC_c = AIC + \frac{2K(K+1)}{n-K-1} \quad (7)$$

336 where AIC is the Akaike Information Criterion as defined by Eq. 4, and K is the
337 number of estimable parameters.

338

339 AIC_c tends to AIC when the number of observations is high relative to the number
340 of calibrated parameters as in our study, where n/K equals 5,081/30 giving 169.

341 Further information criteria were also computed to provide a contrast analysis to
342 the results obtained by the AIC. The BIC (Bayesian Information Criterion) gives a
343 response to the concern that AIC sometimes promotes the use of more
344 parameters than required (Hill and Tidemann, 2007). The BIC is calculated with
345 (Doherty, 2012):

$$346 \quad BIC = n \ln(\hat{\sigma}^2) + p \ln(n) \quad (8)$$

347 The KIC (Kashyap's Information Criterion) additionally considers the likelihood of
348 the parameter estimates in light of their prior values and contains a Fisher
349 information matrix term that imbues it with model selection properties not used by
350 AIC, AICc or BIC. KIC weights and ranks alternative models with respect to the
351 models' predictive performance under cross validation with real hydrologic data
352 (Ye et al., 2008). KIC was derived in the Bayesian context by Kashyap (1982)
353 and is calculated with (Doherty, 2012):

$$354 \quad KIC = (n - (p - 1)) \ln(\hat{\sigma}^2) - (k - 1) \ln(2\pi) + \ln|\mathbf{J}'\mathbf{Q}\mathbf{J}| \quad (9)$$

355

356 *Conceptual Approach*

357 All models were calibrated to the same data set of piezometric pressure heads,
358 and the model with the smallest information criterion is regarded as the optimal
359 one of all proposed models as selected by AIC, AICc, BIC, and KIC, respectively.

360 First, the uncalibrated model using only sedimentological information was
361 simulated (Model 1), then the five most widespread horizontal hydraulic
362 conductivities were estimated (Model 2). In Model 3, all horizontal hydraulic
363 conductivities were considered and vertical hydraulic conductivities were tied by
364 a factor of 0.1 ($K_v = K_H/10$). The next model (Model 4) computed additionally to
365 the horizontal hydraulic conductivity the five most widespread storage
366 coefficients. Model 5 estimated all horizontal conductivities and storage
367 coefficients. In Model 4 and 5 vertical hydraulic conductivities were still tied. Then
368 in Model 6 all horizontal and vertical conductivities were estimated independently
369 and in addition the five most widespread storage coefficients. Finally, Model 7
370 independently estimated all horizontal and vertical hydraulic conductivities and all
371 storage coefficients for all zones of the model domain giving a total amount of 30
372 adjustable parameters (Tab. 1).

373

374 ***Tab 1: Calibrated models analyzed with AIC, AICc, BIC, KIC.***

375

376 Finally, using the paired model methodology (Doherty and Christensen, 2012)
377 the benefit of a more complex model associated with good calibration results
378 versus a simple model yielding a higher certainty is assessed. Simulation results
379 of both models are given against each other in a scatter plot. Coefficients
380 (intercept and slope) of the regression line allow analyzing the bias of the simple
381 versus the results obtained by the optimal and more complex model with a
382 higher degree of freedom and uncertainty.

383 3. Results

384 3.1 Sensitivity Analysis

385 For each observation group time-dependent dimensionless sensitivity coefficients
386 of the measured piezometric pressure heads are shown in Fig. 6. The relative
387 pattern of the sensitivities between the groups is independent from the number of
388 parameters used in the automated model calibration. Sensitivity is always highest
389 for the Northern area as the best optimization results could be obtained for this
390 region. Lowest sensitivities are always computed for observation wells near the
391 River Main and the Jacobi Pond (*Fig. 6*). These low sensitivities display the
392 impact of surface water-groundwater exchange on the groundwater level. In this
393 part of the study area, groundwater levels were mostly driven by the stage
394 of the surface water and leakage through the colmation layer of the river and
395 pond bed sediments and that were not adjusted in the automated model
396 calibration. Hydraulic conductivities of the colmation layers of the Jacobi-pond
397 and Main were derived from a manual “pre-calibration” and fixed with $5 \cdot 10^{-6} \text{ m s}^{-1}$
398 and $1.2 \cdot 10^{-5} \text{ m s}^{-1}$, respectively.

399 Sensitivities of all observation groups follow changes of the groundwater level
400 fluctuations and decrease, when the groundwater extraction stopped in 2005.

401

402 ***Fig. 6: Sensitivity of the six observation groups with respect to the***
403 ***adjustable amount of parameters and the cumulative groundwater***
404 ***extraction at the water works Oberforsthaus.***

405

406 Sensitivities were compared for the seven models differing by the number of
407 adjustable parameters from initially 5 to finally 30 parameters. The PEST
408 optimization with five adjustable parameters revealed highest sensitivity
409 coefficients (*Fig. 5*). Increasing the number of adjustable parameters decreased
410 the sensitivity of the piezometric heads. Therefore, considering a model set-up
411 with large numbers of observation data, the number of adjusted model
412 parameters must be chosen parsimonious to prevent an overparameterization
413 and to maintain the influence of the measured data on the model response.

414

415 **3.2 Comparative Results of the Model Selection Criteria**

416 Four information criteria were computed to select the optimal model approach.
417 Computing the AIC, AICc, BIC, KIC allowed the evaluation of the best conceptual
418 model with respect to complexity and parameter uncertainty. Since Eq. (4) has to
419 be minimized, the lowest information criterion value indicates the best model.
420 Model complexity was gradually increased from the uncalibrated stage (based on
421 sedimentological information) to 30 adjustable model parameters (*Tab. 1*). This
422 increase in complexity was linearly penalized; as expected, by considering more
423 parameters the model fit steadily improved until reaching a constant level with
424 only little further improvement (*Fig. 7*). By comparing the model fit and the penalty
425 against the value of the information criterion the models can be ranked. The
426 scale of the y-axis is omitted in *Fig. 7* since the information criterion is a relative
427 measure and the absolute values are meaningless. Important are, however, the
428 differences to the best model (AIC Δ_j ; BIC Δ_j ; KIC Δ_j ; *Tab 2*)

429 Both, AIC and AICc assess the similar model as optimal. The lowest AIC and
430 AICc value is achieved by Model 4 with 15 adjustable parameters. The selection
431 of AIC and AICc mirrors the trend of the model fit that improved distinctively
432 between Model 1 and Model 4, and stagnated with more than 15 adjustable
433 model parameters. Model 2 (5 adjustable parameters) and Model 7 (30
434 adjustable parameters) were assessed similarly poor due to a lack of model fit to
435 the data (Model 2) or an unjustified complexity (Model 7).

436

437 ***Fig. 7: AIC (diamond), AICc (square), BIC (triangle), KIC (circle) assessment***
438 ***of the calibrated models with respect to complexity and model fit.***

439

440 Relative Akaike weights (AIC w_j), Eq. (4), were computed for all models to
441 express in percent the likelihood of a model, where a likelihood of 100 % means
442 that the corresponding model alone is regarded to represent the “best option”,
443 while a likelihood of 0 % corresponds to a model that has absolutely no support
444 when compared to other models (Tab. 2). In our case, the model selected as
445 optimal (AIC $\Delta_j = 0$) is associated with a likelihood of about 98 %. All other
446 models have practically no support according to the AIC and are either
447 underparameterized (Models 1, 2 and 3) or clearly overparametrized (Models 5, 6
448 and 7).

449

450 ***Tab 2: Differences Δ_j of the AIC, BIC and KIC values to the optimal model,***
451 ***respectively, and likelihood of the flow models from the Akaike***
452 ***weights (AIC w_j).***

453

454 All information criteria (AIC, AICc, BIC, and KIC) selected Model 1 (uncalibrated
455 model based on sedimentological information) as worst model (highest
456 information criteria). However, differences occurred in the selection of the optimal
457 model and model ranking (Fig. 7).

458 The BIC assesses a very simple model, Model 2 with 5 adjustable parameters,
459 as the optimal model and Model 7 (30 adjustable parameters) as unfeasible. BIC
460 values of the different models are varying more pronounced than AIC values
461 differ (Tab. 2). The KIC evaluates Model 3 (10 adjustable parameters) as optimal
462 model and also Model 7 (30 adjustable parameters) as worst model. BIC and KIC
463 choose as best model approaches with fewer adjustable parameters as they
464 assume that in the true model still the prior information exist (Burnham and
465 Anderson, 2004). Thus, they select for greater certainty, which threatens to
466 capture a precise, but less accurate answer than that selected by AIC. Also due
467 to a decreasing sensitivity of the observation data with increasing parameter
468 freedom, Model 3, as selected by KIC, might still provide a valuable model
469 concept with a reasonable precise match of the observation data. Finally, all
470 selection criteria argue against increasing the model complexity to more than 15
471 adjustable parameters.

472 The model based solely on sedimentological information is assessed by all
473 information criteria as worst model. The bias and worth of this simple model can
474 be explored in detail with the paired model methodology as given in Doherty and
475 Christensen (2012). The model output of the simple uncalibrated model is
476 compared against the results of the optimal model selected by the AIC (Fig. 8).
477 The regression coefficients (intercept and slope) of the line through the scatter
478 plot allow addressing effects of simplification on the model predictions. The

479 intercept differs distinctively from zero indicating the null space contribution of the
480 parameter matrix to the prediction error and thus that the simple model possess
481 consistent an error into the predictions (Doherty and Christensen, 2012). The
482 slope of the scatter line is near 1. Hence, parameter surrogacy does not affect
483 the uncalibrated model's ability to predict the piezometric pressure heads. The
484 correlation coefficient of 0.99 indicated that the model based on sedimentological
485 information might give already reasonable results. However, due its null space
486 contribution to the prediction error the uncalibrated model based on
487 sedimentological information can be excluded to provide already a true model.

488

489 ***Fig 8: Paired model analysis: predicted piezometric pressure heads of***
490 ***Model 1 (based on sedimentological information) versus the results***
491 ***of the optimal model selected by AIC (Model 4), regression line***
492 ***equation, and correlation coefficient (R^2).***

493

494 **3.3 Optimization Results**

495 *Obtained residuals*

496 The model calibration was based on piezometric heads measured monthly
497 between 1990 and 2009 in 41 observation wells. Measurements were not
498 available every month at every observation well, giving a total amount of 5,081
499 piezometric pressure head data for the calibration. Computed and measured
500 piezometric heads of the model with the smallest AIC (Model 4) are compared for
501 each observation group in *Fig. 9*.

502 Within the Western area groundwater levels varied over 3 m. This fluctuation
503 resulted from the impact of the water works Goldstein located south of this

504 region. Within the southern part groundwater levels varied up to 2.1 m and also
505 displayed the impact of the water works Goldstein. Around the water works
506 Oberforsthaus groundwater levels varied over a range of 1.2 m. This lower
507 groundwater level drop can be explained by the artificial recharge infiltrated at
508 this water works. Within the Northern area, near the River Main and the Jacobi
509 pond, groundwater levels remained almost constant with only minor fluctuations
510 associated with changes in precipitation and river discharge during the year.

511

512 ***Fig 9: Simulated piezometric heads of Model 4 (optimal model) versus***
513 ***measured piezometric heads between 1990 and 2009. Observation***
514 ***wells were summarized in six groups. One observation well of each***
515 ***group is illustrated within the figure.***

516

517 Within most regions, measured groundwater levels were reasonably well
518 reproduced by the flow model (*Tab. 3, Fig. 9*). The smallest standard error of the
519 weighted residuals was obtained with 0.22 to 0.23 near the Jacobi pond (group 5;
520 *Tab. 3*). Around the water works Oberforsthaus (group 1) and within the Western
521 part (group 4) computed standard errors of the weighted residuals increased to
522 0.47 to 0.51, which can still be assessed as sufficient with respect to the high
523 uncertainties in boundary conditions and model parameter values. Calibration
524 results obtained for observation wells located near the river Main (group 6)
525 showed the highest standard error of the residuals with up to 1.34 that might
526 result from the interpolation of the river stage within the model domain.

527 Six observation wells were used for the model validation containing 1,445
528 observations or 22% of initial available calibration data. Groundwater levels
529 simulated by the optimal model matched measured values at most locations

530 reasonably well (group 1, 4, 5, and 6) and demonstrated that model parameters
531 were estimated within a reliable range (Tab. 3). However, at two locations (group
532 2 and 3) the model fit was distinctively poor and with a similar standard error as
533 obtained with the model based on sedimentological information.

534 In summary, by increasing the amount of adjustable hydraulic conductivities,
535 mean residuals decreased and the standard error of weighted residuals improved
536 from 1.18 (Model using only sedimentological information) to finally 0.74 in Model
537 7 with 30 adjustable model parameters.

538

539 ***Tab 3: Standard error of the weighted residuals of the six observation***
540 ***groups and total sum of squared weighted residuals for each of the***
541 ***seven conceptual models obtained by the inverse PEST model***
542 ***(Model 1 to 7) and with the AIC optimal model (Model 4) during the***
543 ***model validation.***

544

545 *Obtained Parameter Estimates*

546 Very limited information was available from field investigations about hydraulic
547 conductivity and storage. The ratio between vertical and horizontal hydraulic
548 conductivities was assumed to be 1:10 within Models 2, 3, 4. Applying this
549 assumption and additionally calibrating the most widespread storage coefficients
550 (Model 4) was assessed by the AIC as the most certain model with a likelihood of
551 98 %. Hydraulic conductivities were estimated distinctively higher by PEST in
552 most regions than derived from sedimentological information (*Tab. 4*). These
553 differences may result from the impact of secondary flow pathways or local
554 heterogeneities that were missed by the interpretation of the borehole data.

555

556 ***Tab. 4: Comparison of the initial guesses of the hydraulic conductivity***
557 ***based on sedimentological information and values estimated by***
558 ***PEST for the AIC optimal model (Model 4)***

559

560 **4. Concluding Remarks**

561 The investigated combination of model parameters and calibration data could
562 lead to an overparameterized conceptual model. A sensitivity analysis clearly
563 demonstrated that the sensitivity at all observation points decreased by increasing
564 the number of adjustable parameters. This reduced the influence of the field data
565 as constrain for the model predictions. Computing the AIC, AICc, BIC, and KIC
566 allowed the evaluation of the benefit adjusting high numbers of model
567 parameters. The simplest model based on sedimentological information as well
568 as the complex models were rejected by all information criteria since they are
569 likely to be under- or overparameterized. The paired model methodology also
570 displays the high bias possessed by the simple model into the model predictions.
571 Differences prevail in the choice of the optimal model. AIC selects as best model
572 a model of “medium complexity”. It adjusted five of ten storage coefficients and all
573 ten horizontal conductivities, while keeping the vertical conductivities tied by one
574 order of magnitude lower. The results of the optimal model selected by the AIC
575 approximately resemble observed hydraulic piezometric heads, while keeping
576 estimated model parameters at a minimum. The AIC was able to maintain
577 parsimony and makes predictions with a reasonable uncertainty. KIC and BIC
578 give preference to simpler models increasing the model certainty and to maintain
579 prior information. The optimal models selected by BIC and KIC adjusted only five
580 or ten hydraulic conductivities, respectively, while storage coefficients are kept as
581 deduced from the sedimentological investigations. The model fit is unacceptable

582 in the optimal model selected by BIC. The KIC might be able to select the optimal
583 model for an aquifer system that is described by more precise and well-known
584 field data about model parameter than they were available at our study site.
585 However, in situations with poor information about model parameter and
586 boundary conditions the AIC selection should be given preference as it chooses a
587 parsimony model, but with a sufficient freedom to receive an acceptable model fit.
588 The choice made by AIC reflects the data available for calibration better than the
589 optimal models chosen by the KIC and BIC. In our case, where extensive
590 observation data were available, computing the AIC, and eventually the KIC, can
591 improve model confidence, as it avoids an under- or overparameterization of
592 conceptual models for a given data set. However, to decide between the optimal
593 model selected by the AIC and KIC, respectively, the modeler still needs an
594 overview about the data types converted to boundary and initial conditions and
595 model parameters, which is disregarded in the model ranking by all information
596 criteria.

597

598 **Acknowledgements**

599 We thank Elke Duhr and Stefan Pohl (both Hessenwasser GmbH & Co KG) and
600 Sebastián Fernández for preparing and compiling the geological and hydraulic
601 data. Thanks are due to the comments and suggestions of the two anonymous
602 reviewers that helped to improve the manuscript.

603

604

605 **5. References**

606 Akaike, H. 1973. Information theory and an extension of the maximum likelihood
607 principle In: Kotz S, Johnson NL, editors. (1992) Breakthroughs in Statistics,
608 vol. 1: Foundations and basic theory. New York, USA: Springer-Verlag. pp.
609 610-624 ISBN: 0387975-667.

610 Anderle, H.-J. 1968. Die Mächtigkeiten der sandig-kiesigen Sedimente des
611 Quartärs im nördlichen Oberrhein-Graben und der östlichen Untermain-
612 Ebene.- Notizbl. hess. L.-Amt Bodenforsch., 88: 185-196, Wiesbaden.

613 Anderle, H.-J., Golwer, A. 1980. Tektonik. In: Erläuterungen Geol. Kt. Hessen
614 1:25000, Bl. 5917 Kelsterbach, S.50-64, 4 Abb.; Wiesbaden.

615 Bartz, J. 1974. Die Mächtigkeit des Quartärs im Oberrheingraben.- In: Illies, J.H.
616 & Fuchs, K. (eds.): Approaches to Taphrogenesis: 78 - 87, Stuttgart
617 (Schweitzerbarth).

618 Berger, J.-P., Reichenbacher, B., Becker, D., Grimm, M., Grimm, K., Picot, L.,
619 Storni, A., Pirkenseer, C., Derer, C., and Schaefer, A. 2007. Paleogeography
620 of the Upper Rhine Graben (URG) and the Swiss Molasse Basin (SMB) from
621 Eocene to Pliocene: International Journal of Earth Sciences, 94: 697-710.

622 Berthold, G., Hergesell, M. 2005. Flächendifferenzierte Untersuchungen zu
623 möglichen Auswirkungen einer Klimaänderung auf die
624 Grundwasserneubildung in Hessen. INKLIM 2012 - Integriertes
625 Klimaschutzprogramm. Abschlussbericht Hessisches Landesamt für Umwelt
626 und Geologie, Wiesbaden.

627 Bredehoeft, J. D. and Konikow, L. F. 2012. Ground-Water Models: Validate or
628 Invalidate. *Ground Water*, 50 (4): 493–495.

629 Burnham, K.P., Anderson, D.R. 2002. *Model Selection and Multimodel Inference:
630 A Practical Information-Theoretic Approach*, 2nd ed. Springer-Verlag. ISBN 0-
631 387-95364-7.

632 Burnham, K.P., Anderson, D.R. 2004. Multi-model inference: Understanding AIC
633 and BIC model selection. *Sociological Methods and Research*. 33 (2): 261–
634 304.

635 Cavanaugh, J. E. 1997. Unifying the derivations of the Akaike and corrected
636 Akaike information criteria. *Statistics & Probability Letters*, 33: 201-208.

637 Doherty, J. 2012. Addendum to the PEST manual. *Watermark Numerical
638 Computing*: Brisbane, Australia.

639 Doherty, J. 2010. *PEST - Model-Independent Parameter Estimation. User's
640 Manual*, 5th ed.; *Watermark Numerical Computing*: Brisbane, Australia.

641 Doherty, J., Christensen, S. 2012: Use of paired simple and complex models to
642 reduce predictive bias and quantify uncertainty. *Water Resources Research*.
643 47, W12534.

644 Foglia, L., Mehl, S.W., Hill, M.C., Perona, P., Burlando, P. 2007. Testing
645 Alternative Ground Water Models Using Cross-Validation and Other Methods,
646 *Ground Water*, 45(5): 627-641.

647 Harbaugh, A.W. 2005. MODFLOW-2005, the U.S. Geological Survey modular
648 groundwater model - the Ground-Water Flow Process: U.S. Geological Survey
649 Techniques and Methods 6-A16, US.

650 Hill, M. C. 2006. The practical use of simplicity in developing ground water
651 models. *Ground Water*, 44(6):775-81.

652 Hill, M. C., Tiedeman, C. R. 2002. Weighting observations in the context of
653 calibrating groundwater models. IAHS-AISH Publication; 277: 196-203.

654 Hill, M.C., Tiedeman, C.R. 2007. Effective groundwater model calibration - with
655 analysis of data, sensitivities, predictions, and uncertainty. Hoboken, USA:
656 John Wiley & Sons. ISBN: 978-0-471-77636-9.

657 Kashyap, R. L. 1982. Optimal choice of AR and MA parts in autoregressive
658 moving average models, *IEEE Trans. Pattern Anal. Machine Intell.*, 4(2), 99–
659 104.

660 Kazumba, S., Gideon, O., Yusuke, H., Kohji, K. 2008. Lumped model for regional
661 groundwater flow analysis, *Journal of Hydrology*, 359 (1–2): 131-140. Lahner,
662 L., Toloczyki, M. 2004. *Geowissenschaftliche Karte der Bundesrepublik*
663 *Deutschland 1: 2.000.000, Geologie*, Bundesanstalt für Geowissenschaften
664 und Rohstoffe; Hannover.

665 Massmann, C., Birk, S.; Liedl, R; Geyer, T. 2006. Identification of hydrogeological
666 models: application to tracer test analysis in a karst aquifer. In: *Calibration and*
667 *Reliability in Groundwater Modelling: From Uncertainty to Decision Making*
668 *(Proceedings of ModelCARE'2005, The Hague, The Netherlands, June 2005)*
669 *IAHS Publ. 304, 2006.*

670 Parker, A. H., West, L. J., Odling, N. E. and Bown, R. T. 2010. A Forward
671 Modeling Approach for Interpreting Impeller Flow Logs. *Ground Water*, 48: 79–
672 91.

673 Poeter, E.P., Anderson, D.R. 2005. Multimodel ranking and inference in ground
674 water modeling. *Ground Water*, 43(4):597-605.

675 Singh, A., Mishra, S., Ruskauff, R. 2010. Model averaging techniques for
676 quantifying conceptual model uncertainty. *Ground Water*, 48 (5): 701-715.

677 Ye, M., Meyer, P.D., Neuman, S.P. 2008. On model selection criteria in
678 multimodel analysis. *Water Resources Research*, 44(3): W03428.

679 Ye, M., Pohlmann, K. F., Chapman, J. B., Pohl, G. M. and Reeves, D. M. 2010. A
680 Model-Averaging Method for Assessing Groundwater Conceptual Model
681 Uncertainty. *Ground Water*, 48: 716–728.

682 Ziegler, P.A. and Dèzes, P. 2007. Evolution of the lithosphere in the area of the
683 Rhine Rift System: *International Journal of Earth Sciences*, 94: 594-614.

684

685

686

Tab 1: Calibrated models analyzed with AIC, AICc, BIC, KIC.

Model	Number of adjusted parameters during automated model calibration	
	Conductivities	Storage coefficients
1	based on sedimentological data	
2	5	0
3	10	0
4	10	5
5	10	10
6	20	5
7	20	10

687

688

689
690
691

Tab 2: Differences Δ_j of the AIC, BIC and KIC values to the optimal model respectively, and likelihood of the flow models from the Akaike weights (AIC w_j).

Model	AIC Δ_j	BIC Δ_j	KIC Δ_j	AIC w_j
1	4698	4823	4645	0.00
2	37.8	0.0	21.8	0.00
3	10.1	4.9	0.0	0.01
4	0.0	27.5	2.8	0.98
5	8.8	68.9	20.8	0.01
6	18.9	111.8	19.7	0.00
7	29.8	155.3	50.8	0.00

692
693

694
695
696
697
698

Tab 3: Standard error of the weighted residuals of the six observation groups and total sum of squared weighted residuals for each of the seven conceptual models obtained by the inverse PEST model (Model 1 to 7) and with the AIC optimal model (Model 4) during the model validation.

Model	Standard error of weighted residuals [-]						
	G1	G2	G3	G4	G5	G6	Total Residual
1	0.734	1.966	0.752	0.728	0.265	1.393	1.18
2	0.472	0.640	0.499	0.494	0.219	1.341	0.750
3	0.470	0.607	0.628	0.503	0.233	1.306	0.745
4	0.475	0.602	0.591	0.507	0.225	1.317	0.745
5	0.473	0.599	0.636	0.509	0.234	1.307	0.744
6	0.473	0.600	0.628	0.508	0.234	1.305	0.744
7	0.472	0.613	0.574	0.508	0.217	1.306	0.743
Validation	0.397	0.844	0.990	0.509	0.317	1.092	-

699

700 Group 1: Around water works *Oberforsthaus*
 701 Group 2: Southern area
 702 Group 3: Northern area
 703 Group 4: Western area
 704 Group 5: Near Jacobi Pond
 705 Group 6: Near river Main
 706 Total residuals: obtained for 5,081 piezometric pressure head data
 707 Validation: Residuals obtained for 1,445 piezometric pressure head data with the optimal
 708 model (Model 4)

709

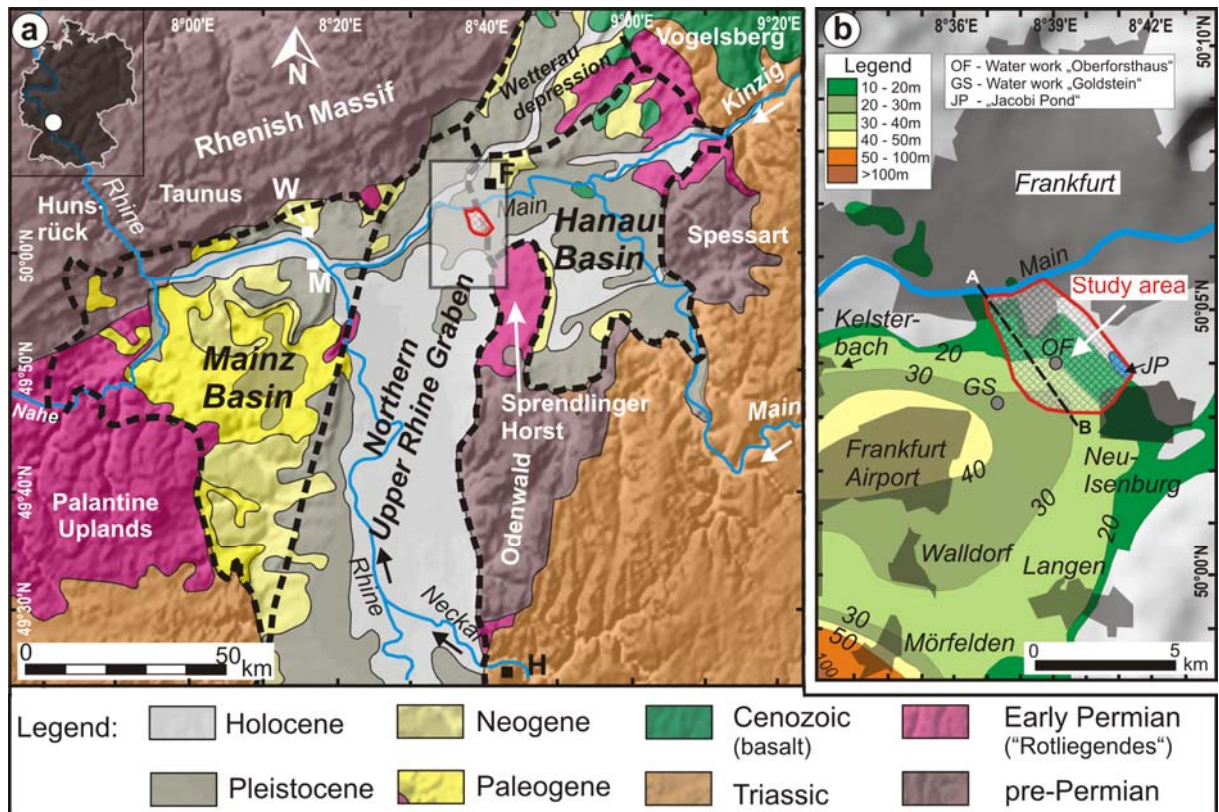
710

711
712
713

Tab 4: Comparison of the initial guesses of the hydraulic conductivity based on sedimentological information and values estimated by PEST for the AIC optimal model (Model 4)

Zone	Hydraulic conductivity [m/s]			
	Horizontal		Vertical	
	<i>Estimated from sedimentological information</i>	<i>Estimated by PEST</i>	<i>Estimated from sedimentological information</i>	<i>Estimated by PEST</i>
1	$5.6 \cdot 10^{-3}$	$1.7 \cdot 10^{-1}$	$5.6 \cdot 10^{-4}$	$1.7 \cdot 10^{-2}$
2	$3.8 \cdot 10^{-3}$	$4.8 \cdot 10^{-1}$	$3.8 \cdot 10^{-4}$	$4.8 \cdot 10^{-2}$
3	$5.3 \cdot 10^{-3}$	$1.5 \cdot 10^{-1}$	$5.3 \cdot 10^{-4}$	$1.5 \cdot 10^{-2}$
4	$6.8 \cdot 10^{-3}$	$3.5 \cdot 10^{-2}$	$6.8 \cdot 10^{-4}$	$3.5 \cdot 10^{-3}$
5	$8.3 \cdot 10^{-3}$	$5.7 \cdot 10^{-3}$	$8.3 \cdot 10^{-4}$	$5.7 \cdot 10^{-4}$
6	$9.8 \cdot 10^{-3}$	$1.8 \cdot 10^{-2}$	$9.8 \cdot 10^{-4}$	$1.8 \cdot 10^{-3}$
7	$1.1 \cdot 10^{-2}$	$2.0 \cdot 10^{-2}$	$1.1 \cdot 10^{-3}$	$2.0 \cdot 10^{-3}$
8	$1.3 \cdot 10^{-2}$	$6.8 \cdot 10^{-2}$	$1.3 \cdot 10^{-3}$	$6.8 \cdot 10^{-3}$
9	$1.4 \cdot 10^{-2}$	$6.6 \cdot 10^{-2}$	$1.4 \cdot 10^{-3}$	$6.6 \cdot 10^{-3}$
10	$1.0 \cdot 10^{-7}$	$4.3 \cdot 10^{-7}$	$1.0 \cdot 10^{-8}$	$4.3 \cdot 10^{-8}$

714

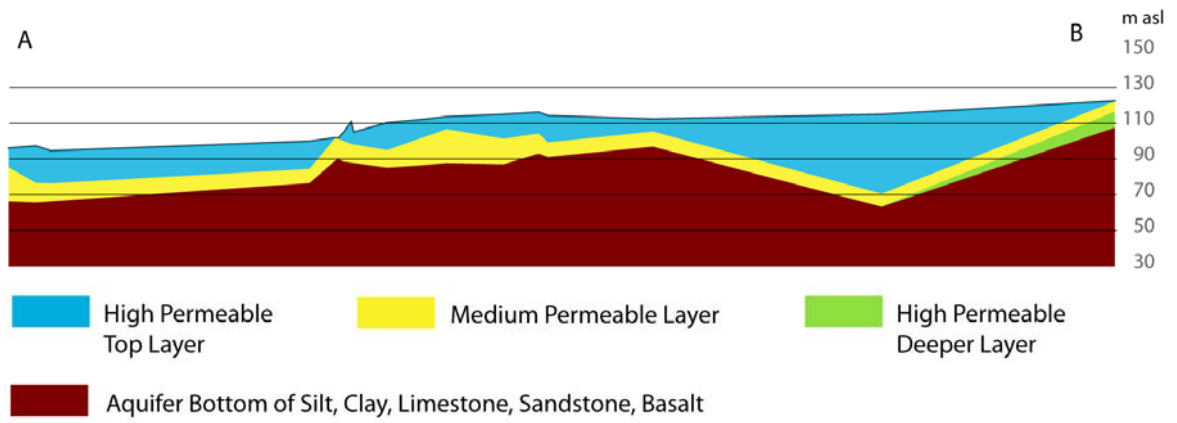


715

716 **Fig. 1: a) Simplified geological map showing the northern part of the Upper**
 717 **Rhine Graben, the adjacent Mainz and Hanau basins (modified after**
 718 **Lahner and Toloczyki (2004); W: Wiesbaden, M: Mainz, F: Frankfurt, H:**
 719 **Heidelberg). b) Thickness of the Quaternary sand and gravel deposits**
 720 **south of Frankfurt (after Anderle, 1968; Bartz, 1974; Anderle and**
 721 **Golwer, 1980). Location of the model domain, the water works, and of**
 722 **transect A-B.**

723

724



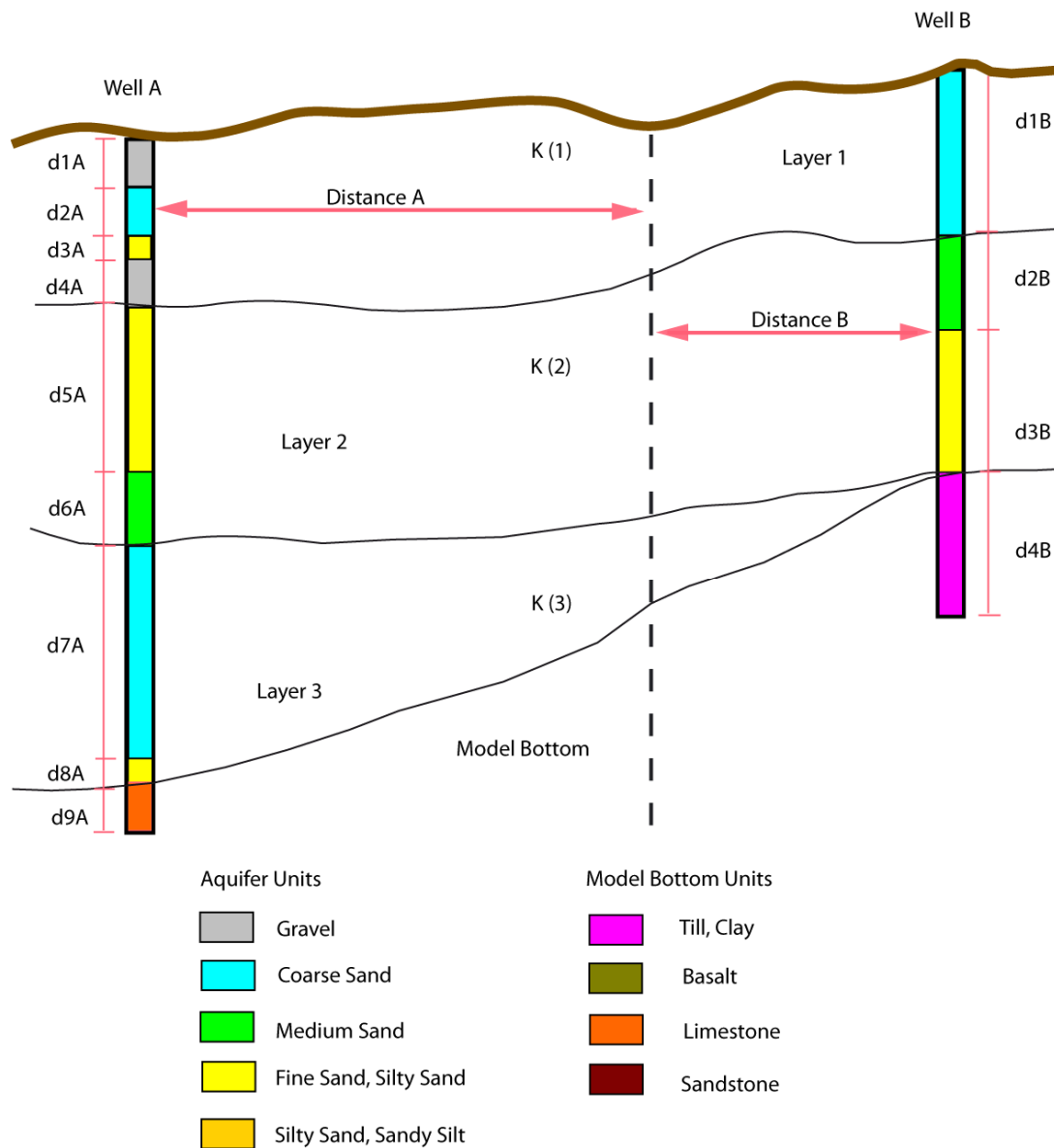
725

726

727

728

Fig 2: Averaged hydrostratigraphic layer from nine lithologic units along transect A-B.



729

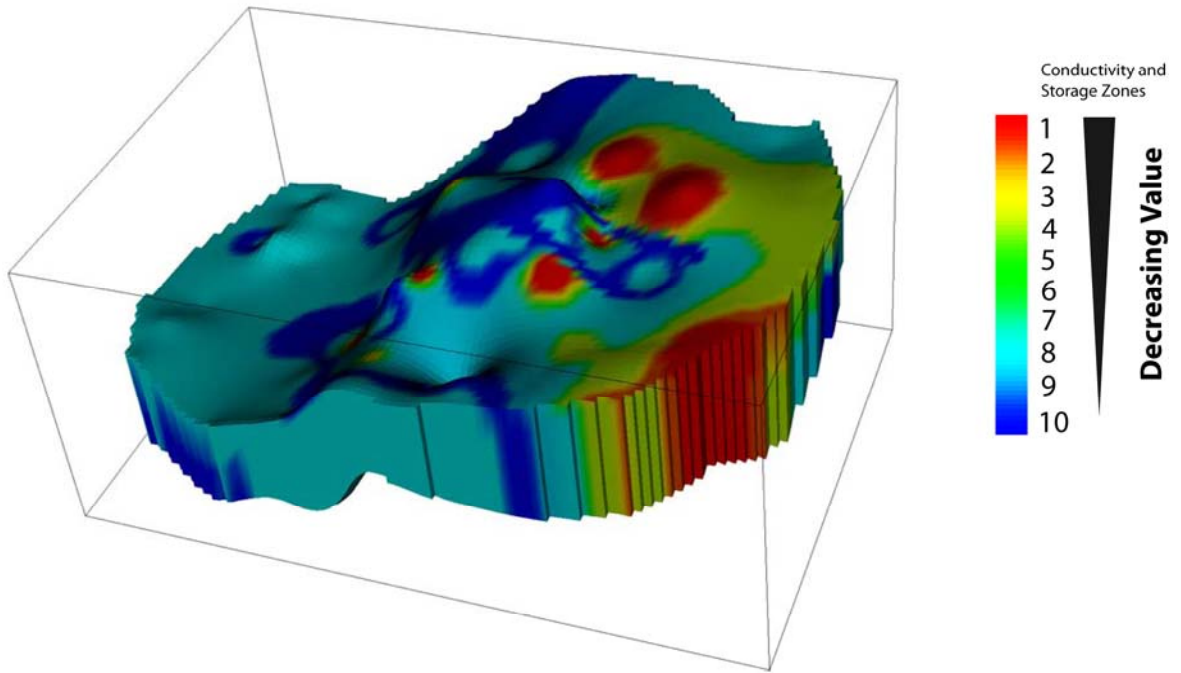
730

731

732

733

Fig 3: Averaging technique to derive the equivalent hydraulic conductivities around two wells within the three hydrostratigraphic layer that contain nine lithologic units.



734

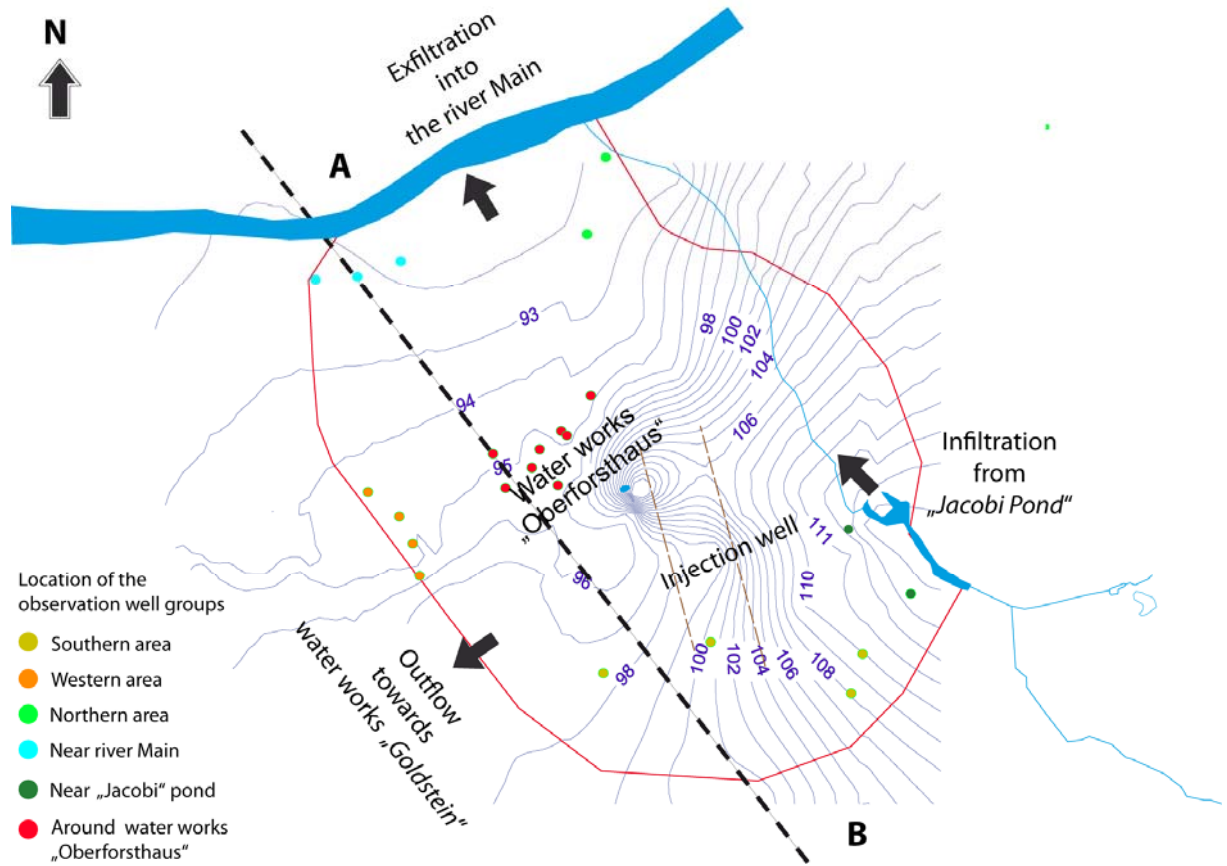
735

736

737

738

Fig 4: Spatial distribution of the ten equivalent hydraulic conductivities of Model 1 (uncalibrated model based on sedimentological information) within the three hydrostratigraphic layer.



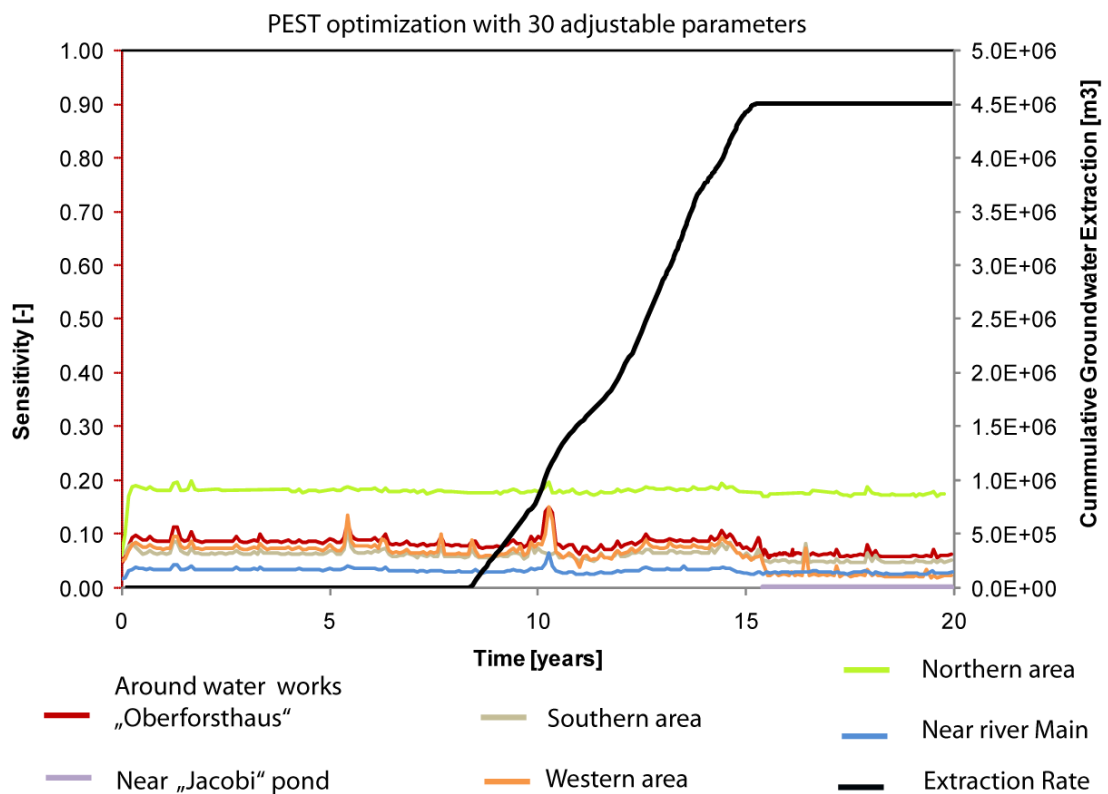
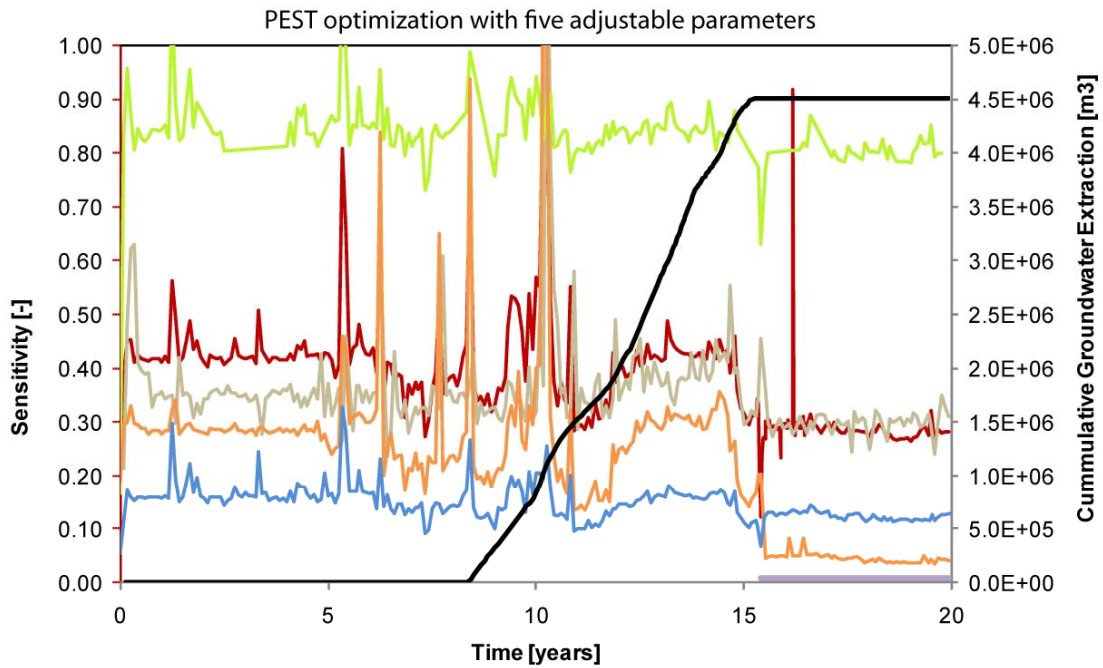
739

740

741

742

Fig 5: Boundary conditions, initial head distribution of the numerical flow model and location of the observation well groups.



- Around water works „Oberforsthaus“
- Southern area
- Northern area
- Near „Jacobi“ pond
- Western area
- Near river Main
- Extraction Rate

743

744

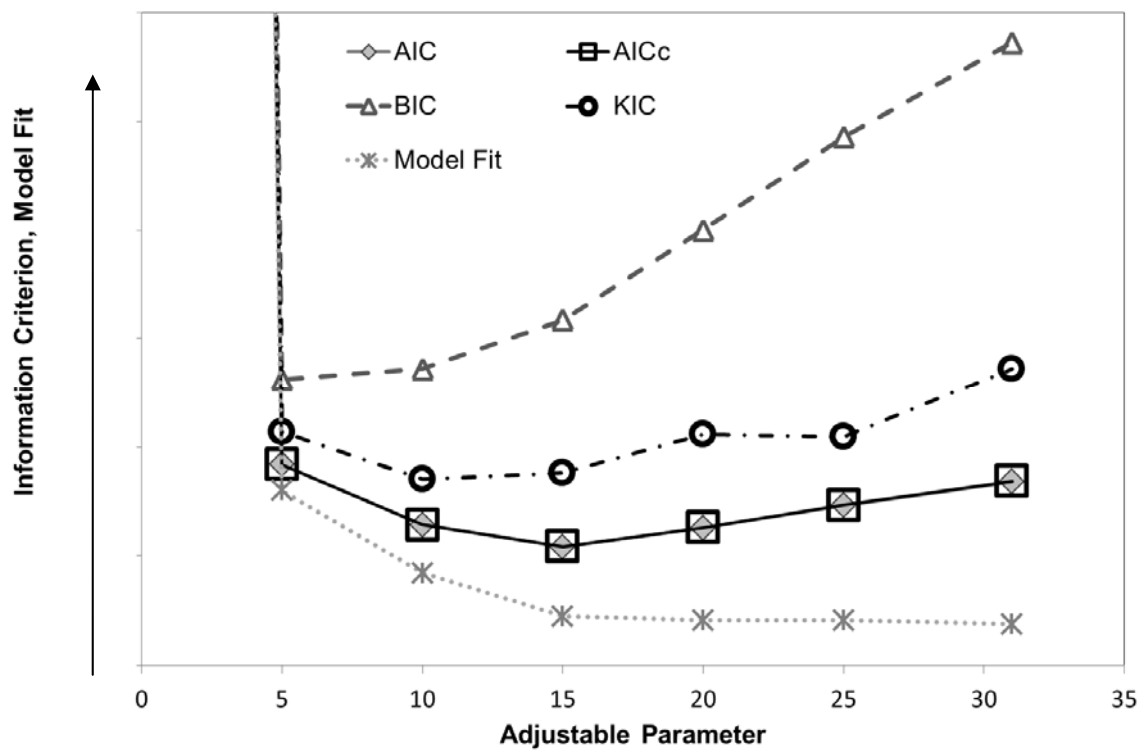
745

746

747

Fig 6: Sensitivity of the six observation groups with respect to the adjustable amount of parameters and the cumulative groundwater extraction at the water works Oberforsthaus.

748

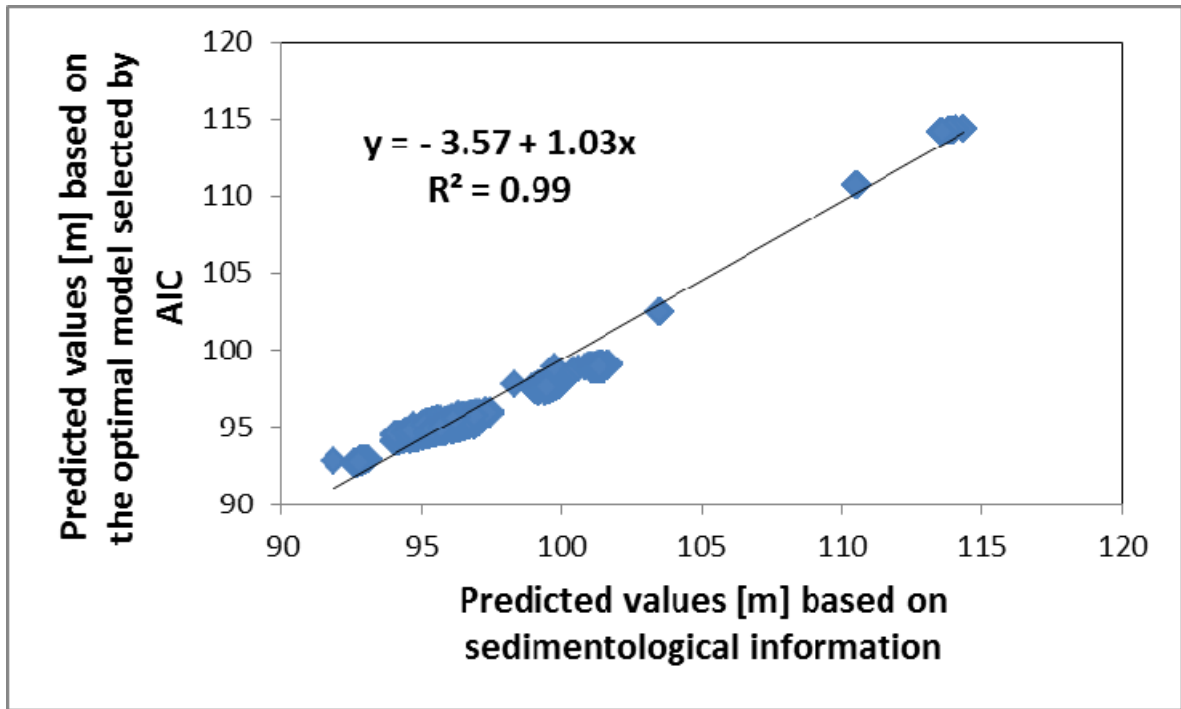


749

750 **Fig 7: AIC (diamond), AICc (square), BIC (triangle), KIC (circle) assessment**
751 **of the calibrated models with respect to complexity and model fit.**

752

753

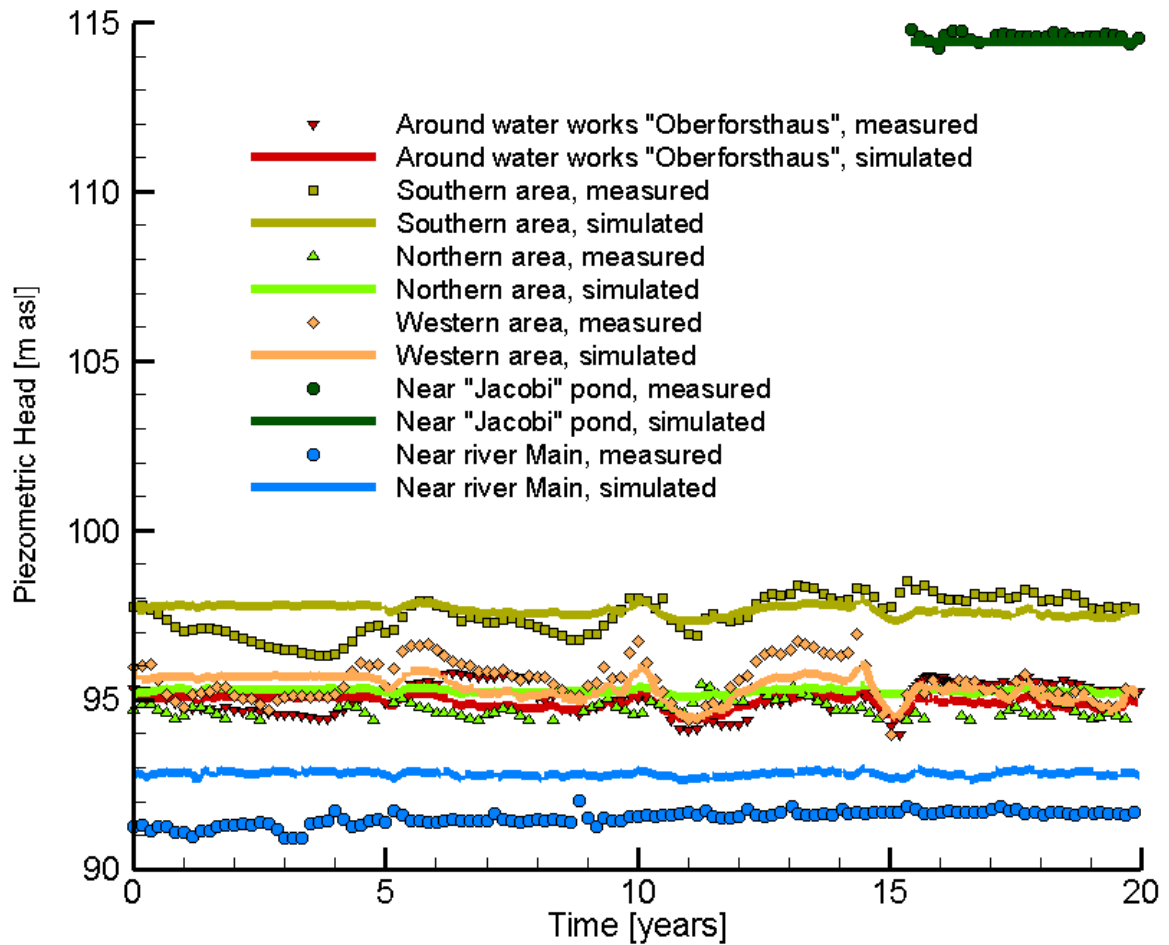


754

755 **Fig 8: Paired model analysis: predicted piezometric pressure heads of**
 756 **Model 1 (based on sedimentological information) versus the results**
 757 **of the optimal model selected by AIC (Model 4), regression line**
 758 **equation, and correlation coefficient (R^2).**

759

760



761

762

763

764

765

Fig 9: Simulated piezometric heads of Model 4 (optimal model) versus measured piezometric heads between 1990 and 2009. Observation wells were summarized in six groups. One observation well of each group is illustrated within the figure.